Genes & Genomics
https://doi.org/10.1007/s13258-025-01715-x

Online ISSN 2092-9293
Print ISSN 1976-9571

ORIGINAL ARTICLE

Deciphering the molecular landscape of hepatopancreatic necrosis disease in *Eriocheir sinensis* using RNA-Seq meta-analysis

Adeel Malik[1] · Nitin Mahajan[2] · Hyung-Eun An[1,3] · Chang-Bae Kim[3]

Received: 5 June 2025 / Accepted: 9 November 2025

Abstract

Background The Chinese mitten crab (*Eriocheir sinensis*) is a commercially important crustacean, highly valued in China and Korean peninsula for its nutritional benefits and delicate flavor. However, the aquaculture industry has been significantly impacted by hepatopancreatic necrosis disease (HPND), leading to substantial economic losses. The exact cause and molecular mechanisms underlying HPND remain poorly understood.

Objective This study aimed to decipher the genetic and molecular basis of HPND through an integrative transcriptomic meta-analysis to identity consistent and disease related gene expression patterns.

Methods Publicly available RNA-Seq datasets from three different studies were systematically integrated and analyzed. Differentially expressed transcripts (DETs) were identified through meta-analysis, followed by functional annotation and enrichment analyses of Gene Ontology and KEGG pathways.

Results The meta-analysis identified 571 DETs, including 245 up-regulated and 326 down-regulated transcripts in diseased hepatopancreas. Functional enrichment revealed significant disruptions in the pathways of protein modification, lipid metabolism, and vesicle-mediated transport. These processes are crucial for immune functions including pathogen detection, antigen presentation, cytokine secretion, and metabolic adaptation to stress in the hepatopancreas. Moreover, we found 11 novel DETs (6 up-regulated and 5 down-regulated), highlighting the ability of meta-analysis to uncover low-abundance or context-specific genes that may escape detection in individual studies.

Conclusions Our study provides valuable insights into the causes and pathogenic mechanisms of HPND, identifies novel genetic factors and gene markers for detection, and offers a deeper understanding of the disease, highlighting potential biomarkers for its prevention in *E. sinensis* aquaculture.

Keywords *Eriocheir sinensis* · Chinese mitten crab · RNA-Seq · Meta-analysis · Hepatopancreatic necrosis disease · Aquaculture

Introduction

Eriocheir sinensis, commonly known as Chinese mitten crab (CMC), is a freshwater crustacean native to China. It has also become an invasive species in both United States (US) and Europe (Anger 1991). In addition to China, this crab is one of the most important and cost-efficient species for freshwater aquaculture in Korean Peninsula and Eastern Pacific coast (Sui et al. 2009). *E. sinensis* is a unique crustacean that it requires two distinct environmental conditions to complete its life cycle. As an adult, this crab lives in freshwater but migrates to brackish (saline) water for reproduction (Zhang et al. 2018). They are highly valued in China's aquaculture industry due to their rapid growth, high productivity and rich nutritional content (Hong et al. 2019).

Adeel Malik, and Nitin Mahajan have contributed equally to this work.

✉ Adeel Malik
adeel@procarb.org

✉ Chang-Bae Kim
evodevo@smu.ac.kr

[1] Institute of Intelligence Informatics Technology, Sangmyung University, Seoul 03016, Republic of Korea

[2] Freelancer Data Scientist, Saint Louis, MO 63026, USA

[3] Department of Biotechnology, Sangmyung University, Seoul 03016, Republic of Korea

Published online: 26 November 2025

Recognized for their nutritional benefits, flavor, and taste, these crabs have become one of the most economically significant crab species in China and the Korean Peninsula, with an annual production of 808,293 tons in 2021 (FAO, 2024). However, over the last few decades, the rapid expansion of intensive crab farming has led to significant economic losses due to diseases associated with high stocking densities (Wang et al. 2019). Among these diseases, hepatopancreatic necrosis disease (HPND, "shuibiezi" in Chinese) has gained prominence, causing high mortality rates (Ding et al. 2016; Liu et al. 2017; Wang et al. 2021). Clinical symptoms of HPND include discoloration of the hepatopancreas from orange-yellow to pale yellow or grayish white, muscle atrophy and edema (Yang et al. 2020). Affected crabs, while do not die immediately, lose their economic value. Additional symptoms include pale hepatopancreas, water-filled abdominal cavity, black, thin, and brittle shells, and nearly empty stomach and intestine (Chen et al. 2017).

Despite extensive research, the exact cause of HPND in *E. sinensis* remains unclear. Initially, the microsporidian fungus *Hepatospora eriocheir* was thought to be responsible for HPND due to its damage to the hepatopancreas and subsequent metabolic and immune disruptions (Ding et al. 2016). However, later studies found no evidence implicating microorganisms, such as bacteria, fungi, or viruses, in diseased crabs. Furthermore, HPND symptoms failed to manifest when healthy crabs were exposed to infected tissues. These findings suggest that environmental factors such as high-water pH may play a more significant role than pathogens (Pan et al. 2017). Other studies have suggested bacterial imbalances rather than microsporidia or viruses as potential contributors to HPND (Shen et al. 2017). Additionally, metabolic abnormalities, including issues with fatty acid metabolism and high levels of fungicide propamocarb in diseased crabs, further supported a link to environmental stressors (Gao et al. 2018a, b). Yang et al. (2018) also found no pathogens but proposed that non-living agents could be the cause. Overall, while environmental factors appear to be critical, the exact cause of HPND remains unknown, therefore highlighting the need for further research to identify causative agents and develop effective control measures.

Regardless of the causative factors, transcriptional responses to external stimuli are both rapid and sensitive. Changes in the gene expression may provide insights into how crabs respond to specific stressors (Olsvik et al. 2007). Previous transcriptomic studies on crustacean hepatopancreas have shown variability in findings, with gene expression influenced by physiological states, environmental stress, or pathogen exposure. For instance, the hepatopancreas transcriptome of *Portunus trituberculatus* exhibits diverse gene expression patterns linked to growth and ovarian development (Wang et al. 2014). Similarly, research on *Procambarus clarkii* identified 2,497 differentially expressed transcripts (DETs) responding to immune challenges, emphasizing immune and metabolic pathway enrichment. Dietary factors also significantly influenced gene expression in the *E. sinensis*, particularly affecting lipid and carbohydrate metabolism pathways (Dai et al. 2017; Guo et al. 2019). These findings contrast with stress-induced transcriptomic changes in *Macrobrachium rosenbergii*, where immune response and detoxification pathways were predominant (Guo et al. 2019; Liu et al. 2021). In *Litopenaeus vannamei*, transcriptomic studies under cold stress conditions identified significant changes in energy metabolism and oxidative stress pathways, findings distinct from transcriptomic profiles under normal conditions or during disease challenges in other species (Fan et al. 2019).

Although the transcriptome of diseased hepatopancreas has been extensively studied, these findings might not reflect transcriptomic alterations associated with diverse dysfunctions of the organ. For instance, Yang et al. (2020) linked hepatopancreatic necrosis disease (HPND) to pyrethroid exposure; however, their study focused mainly on a single environmental factor, overlooking the multifactorial nature of hepatopancreatic impairment where pathogens, pollutants, and physiological stressors likely interact. Similarly, Chen et al. (2017) reported only 69 differentially expressed genes, limiting both statistical robustness and biological interpretation, as pathway enrichment or systems-level analyses were not performed. Li et al. (2013) investigated responses to three pathogens and provided valuable insight into pathogen-induced immune responses, yet did not consider additional influences such as dietary, environmental, or metabolic stress. Collectively, these studies offer useful perspectives on specific conditions but fall short of depicting an integrated molecular landscape of hepatopancreatic dysfunction.

To address these gaps, the present study performs a comprehensive meta-analysis of publicly available RNA-Seq datasets focused on the hepatopancreas of *E. sinensis*, with particular attention to conditions associated with HPND (Fig. 1). By integrating transcriptomic data from three independent experiments, we aim to identify consistent gene expression patterns, key biological pathways, and potential biomarkers that underpin hepatopancreatic health and disease. This meta-analytic approach overcomes the limitations of small sample sizes in individual RNA-Seq studies—enhancing statistical power, improving reproducibility, and enabling the detection of shared molecular signatures across diverse stressors (Marot et al. 2020; Toro-Domínguez et al. 2021; Cho et al. 2016; Piras et al. 2019). Furthermore, by comparing datasets across different pathological and environmental contexts, we seek to uncover both conserved and context-specific gene expression patterns that are not

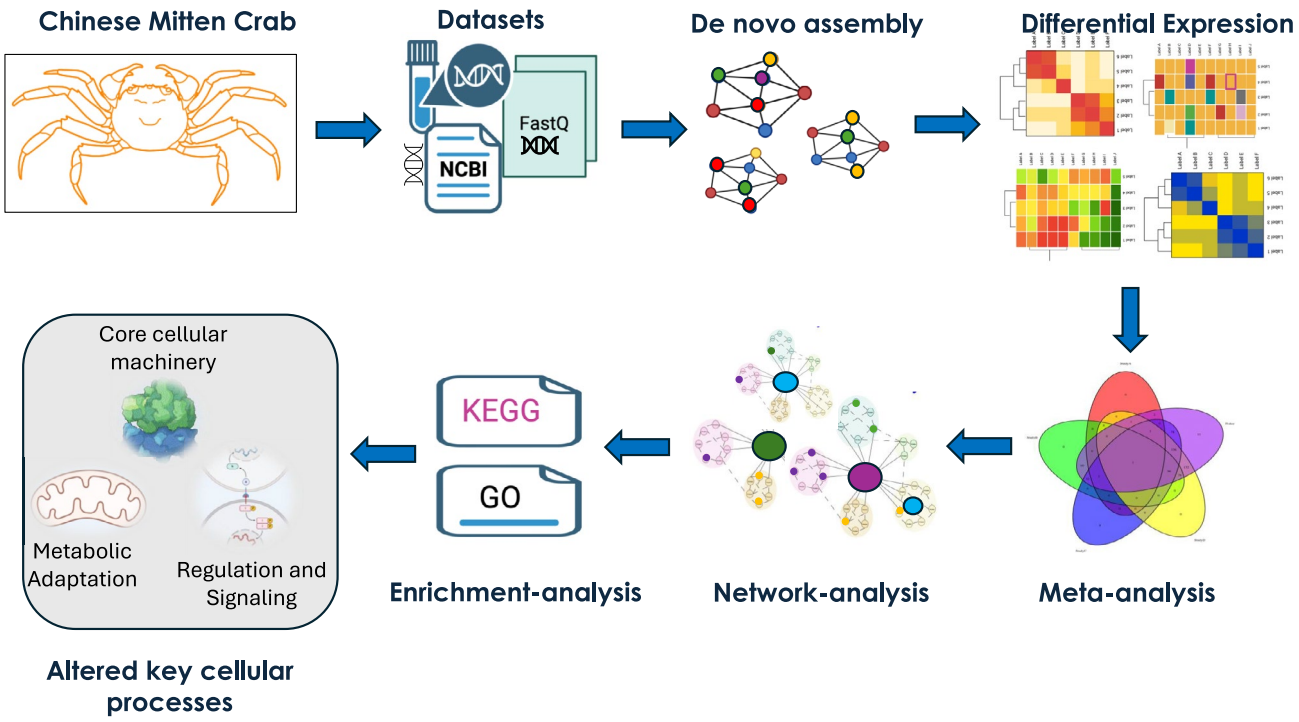

Fig. 1 Schematic overview of the meta-transcriptome analysis workflow for *Eriocheir sinensis*. RNA-seq datasets were retrieved from the NCBI database and assembled de novo. Differential expression analysis was performed to identify key genes, followed by a meta-analysis to detect consistent expression patterns across datasets. Network and pathway analyses (GO and KEGG) were then conducted to uncover functional modules and enriched biological pathways associated with core cellular machinery, metabolic adaptation, and regulatory signaling

Table 1 Overview of the datasets and the number of trimmed reads retained post-filtering

Dataset	Condition	Raw Reads	Trimmed Reads	Reads Retained Post-filtering (%)	References
Study A	White hepatopancreas syndrome	368,111,382	286,145,522	77.73	(Chen et al. 2017)
Study B	Hepatopancreatic necrosis disease (HPND)	427,883,286	416,360,578	97.30	(Yang et al. 2020)
Study C	Microbial Challenged Mitten Crab	206,557,731	173,259,260	83.88	(Li et al. 2013; Chen et al. 2017)
Study D	Microbial Challenged Mitten Crab	313,629,052	310,912,187	99.13	(Li et al. 2013; Yang et al. 2020)

apparent in isolated analyses. To our knowledge, this is the first RNA-Seq meta-analysis to systematically investigate transcriptomic alterations in the diseased hepatopancreas of *E. sinensis*. Our findings provide new insights into the molecular mechanisms driving hepatopancreatic dysfunction and offer a foundation for improved disease management and aquaculture sustainability.

Materials and methods

Datasets

The National Center for Biotechnology Information (NCBI) BioProject (https://www.ncbi.nlm.nih.gov/bioproject) database was utilized to identify RNA-Seq-based studies focusing on the diseased hepatopancreas of the *E. sinensis*. The raw sequencing reads for the selected samples were downloaded as fastq files from the NCBI's sequence read archive (SRA: https://trace.ncbi.nlm.nih.gov/Traces/sra/) using the fastq-dump tool from the SRA Toolkit (http://ncbi.github.io/sra-tools/). Table 1 summarizes the final datasets used in this study.

De novo assembly of RNA-Seq datasets

Prior to assembly, the raw reads were processed using Trimmomatic (Bolger et al. 2014), integrated within the Trinity v.2.15.1 (Haas et al. 2013) pipeline, to filter the reads by removing the adapter sequences, and then, scanning the reads with a 4-base-wide sliding window, trimming regions where the average quality per base dropped below 20. Furthermore, the reads were also discarded if their lengths were reduced below 50% of the original read length. De novo transcriptome assembly was performed on the quality filtered reads by using the Trinity v2.15.1 Docker image, and each dataset was assembled independently.

Assembly statistics and completeness

Assembled transcripts might not always fully represent properly paired-end reads, as some transcripts may be fragmented or short, leading to only one fragment of a pair aligning (Haas et al. 2013). To evaluate the composition of reads in our assembly, we aimed to capture and count all reads that mapped to the assembled transcripts, including both properly paired reads and those that were unpaired. Therefore, Bowtie2 (Langmead and Salzberg 2012) was used to align reads to the transcriptome, and the number of properly paired and unpaired alignments were recorded. BUSCO v.4.0.6 (Seppey et al. 2019) was used to assess the transcriptome completeness of all datasets against the arthropoda_odb10 (https://busco.ezlab.org/frames/art) lin eage as a reference. Transcript abundance was quantified using kallisto, an ultra-fast alignment-free method (Bray et al. 2016) bundled within the Trinity Docker image.

Functional annotation of the transcripts and enrichment analysis

Potential coding regions and open reading frames (ORFs) were predicted with the TransDecoder (Haas, BJ. https://github.com/TransDecoder/TransDecoder) pipeline with the default settings. Redundant sequences were removed using CD-HIT v4.6.8 (Fu et al. 2012). The resulting protein sequences were scanned against the UniProtKB/Swiss-Prot (UniProt Consortium 2019) database using BLASTp (Camacho et al. 2009) implemented via Diamond v2.1.9.163 (Buchfink et al. 2021). Orthologous groups were identified through the eggNOG-mapper (Huerta-Cepas et al. 2017), an online functional annotation tool. Enrichment analysis of gene ontology (GO) terms and KEGG pathways of the differentially expressed transcripts (DETs) was performed using KOBAS-I (Bu et al. 2021) webserver. Only categories with a corrected *p-value* of <0.05 cutoff were considered enriched.

Differential expression and transcriptome meta-analysis

Differential expression (DE) analysis for each study was performed at the isoform level using the edgeR (Robinson et al. 2010) package within the Trinity pipeline. The DE results from all datasets were then combined for a meta-analysis using the metaRNASeq (Rau et al. 2014) package, which applies Fisher's combined probability test (Fisher 1992). Fisher' method combines p-values for each gene across individual studies using the following formula:

$$fg = -2\sum s = 1s \ln\left(pgs\right)$$

where, pgs corresponds to the raw *p*-value calculated for a gene (g) in a differential analysis for the study (s).

Transcripts (genes) with an FDR <0.05 and an average fold change (FC) of ≥ 2 ($\log2FC \leq -1$ or $\log2FC \geq 1$) were classified as DETs in the meta-analysis. Visualization, including heatmap was generated using the pheatmap (https://cran.r-project.org/package=pheatmap) package within the R programming environment (https://www.r-project.org/).

Network analysis and community detection

The amino acid sequences of the DETs were mapped to the STRING v.12.0 (Szklarczyk et al. 2023) database to predict the potential interactions among them. STRING is a comprehensive protein–protein interaction (PPI) database that integrates both experimental data and computational predictions to identify functional associations. The mapping process utilized high-confidence interaction scores, filtering interactions with a combined confidence score of ≥ 0.7 to focus on reliable associations. This threshold ensures that the resulting network reflects biologically meaningful interactions relevant to the hepatopancreatic disease context. The interaction network of the DETs was visualized and analyzed using Cytoscape v.3.8.0 (Shannon et al. 2003). Cytoscape enables detailed exploration and annotation of complex networks, which is critical for identifying key players and interaction hubs within the DET network. Network topology was characterized using the NetworkAnalyzer plugin (Assenov et al. 2008), which computes fundamental metrics such as node degree. Such metrics provide insight into the structure of the network, highlighting central nodes with a high degree of connectivity that may represent critical regulatory elements. To identify distinct functional modules within the PPI network, the GLay plugin (Su et al. 2010) was employed for community detection. GLay implements the modularity-based clustering algorithm, which groups nodes into communities based on their interaction patterns. This approach helps to reveal tightly

connected subgroups that may correspond to specific biological processes or pathways.

Results

Description of the datasets

Based on the search criteria outlined in the methods section, three RNA-Seq datasets related to diseased hepatopancreas of *E. sinensis* were retrieved from the NCBI database (Table 1). These datasets are briefly described as follows:

i. Study A: This study compared gene expression profile of the hepatopancreas in CMC exhibiting white hepatopancreas syndrome with those in normal (yellow) hepatopancreas (Chen et al. 2017).
ii. Study B: This study analyzed the transcriptome differences of the hepatopancreas of CMCs with and without HPND (Yang et al. 2020).
iii. Study C: This study investigated the hepatopancreas transcriptome of CMCs infected with a mixture of three pathogenic strains (*Micrococcus luteus*, *Vibrio alginolyticus* and *Pichia pastoris*). The primary objective of the study was to annotate functional genes and identify potential immune molecules involved in various signaling pathways (Li et al. 2013). A limitation of this study was the absence of control samples. To address this, control datasets from study A were used.
iv. Study D: This dataset is same as Study C (Li et al. 2013); however, control datasets from Study B were used instead of those from Study A.

De novo transcriptome assembly

Each dataset was assembled individually, and Table 1 summarizes the basic assembly statistics for reads from each dataset. To evaluate composition of reads in our assembly, we calculated the proportion of reads that mapped back to the assembled transcripts. The mapping rates ranged from 95–96% (Table S1), which is above 80% threshold and signify a good quality assembly (Haas et al. 2013). The average contig length for all the datasets ranged between 988 and 1079 bp. The N50 value was lowest for Study C (1826), and highest for Study D (2129), suggesting differences in assembly quality. The completeness of the assembled transcripts using BUSCO showed the percentage of orthologs among the Arthropods represented in our assembled CMC transcriptomes. Of the 1013 BUSCO groups analyzed, a high percentage (92–94%) of complete orthologs were identified in each dataset (Table S2). This includes both the complete single-copy ortholog and complete duplicates (putative paralogs or complete genes with multiple copies). For non-model organisms such as *E. sinensis*, BUSCO scores within the range of 50–95% are expected (Seppey et al. 2019).

Identification of coding regions and functional annotation

The TransDecoder pipeline identified 316,596, 368,325, 251,360, and 320,069 transcripts with the longest open reading frames (ORFs) for four datasets, respectively. Each identified ORF was at least 100 amino acids long, and sequences shorter than 100 residues were excluded from further analysis. To remove potential duplicates, the datasets were filtered using CD-HIT, removing the redundant sequences with 100% similarity. Filtration resulted in 138,410, 167,283, 118,474, and 149,413 sequences in each dataset, respectively. This redundancy reduced datasets were then used for functional annotation. Based on the BLASTp search, 20.71%, 26.42%, 23.06%, and 27.65% of sequences from studies A–D, respectively, mapped to the UniProt database. These mapping rates are consistent with, and in some cases, they are comparable to the previous studies on this non-model organism (Malik et al. 2021; Yang et al. 2019). These data suggest that many of the CMC transcripts could be novel and are not represented in the current databases.

Meta-analysis of CMC hepatopancreas transcriptome

Following the DE analysis of each individual dataset, Fisher's method was applied, identifying 571 transcripts with an average fold change of ≥ 2 ($\log 2FC \leq -1$ or $\log2FC \geq 1$) and an adjusted p-vaue of < 0.05. Several transcripts were excluded from the analysis because of their inconsistent or conflicting expression patterns. Among these 571 DETs, 245 transcripts were up-regulated and 326 were down-regulated when the diseased hepatopancreas of the CMCs were compared with the normal hepatopancreas. These 571 DETs were used for further downstream analysis. Figures 2 and 3 provide the overview of top 20 up- and down-regulated transcripts, and the complete list of 571 transcripts with detailed annotations is provided as additional information in Table S3. Notably, the membrane-associated protein Hem is the topmost up-regulated transcript, whereas the most down-regulated transcript encoded endoglucanase A.

Additionally, the p-value combination approach using Fisher's technique identified 11 new transcripts that were not found in individual studies (Fig. 4). Among these, only eight exhibited an average $\log2FC \geq 2$ (Table 2).

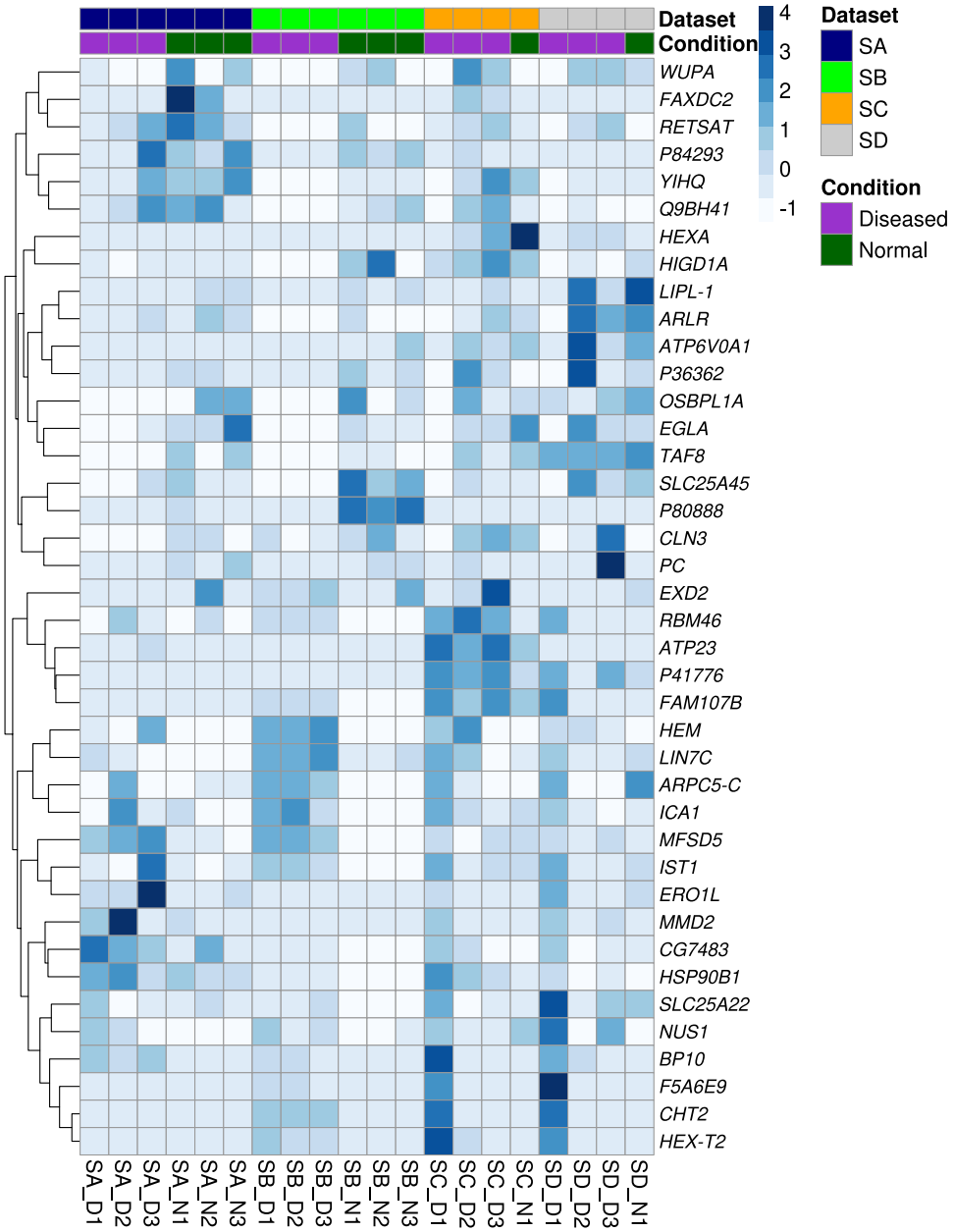

Fig. 2 Heatmap showing top 20 up-regulated and down-regulated transcripts identified by meta-analysis in the diseased hepatopancreas of Chinese mitten crabs. Only transcripts with an average fold change (FC) of ≥ 2 and a Benjamini–Hochberg adjusted *p*-value of < 0.05 were considered to be differentially expressed

Enrichment analysis of DETs based on KEGG pathways and gene ontology

KEGG enrichment analysis identified 36 significantly enriched pathways, mainly grouped into amino acid metabolism, carbohydrate metabolism, lipid metabolism, and energy metabolism (Table S4). A total of 181 DETs were mapped to these pathways—116 down-regulated and 65 up-regulated. The most enriched pathways included glycosphingolipid biosynthesis (ganglio series), synthesis and degradation of ketone bodies, glycosphingolipid biosynthesis (globo and isoglobo series), and butanoate metabolism (Fig. 5).

Although both up- and down-regulated transcripts mapped to overlapping pathways, their distribution patterns differed. Pathways related to lipid and amino acid metabolism (e.g., fatty acid metabolism, glycerophospholipid metabolism, cysteine and methionine metabolism) were dominated by down-regulated transcripts, while endocytosis and fructose and mannose metabolism showed a predominance of up-regulated genes (Fig. 6). Notably, ten KEGG pathways were exclusively enriched with down-regulated transcripts, including lysosome and beta-alanine metabolism.

GO enrichment analysis of 571 DETs revealed 83 significantly enriched terms across biological processes (BP), molecular functions (MF), and cellular components (CC)

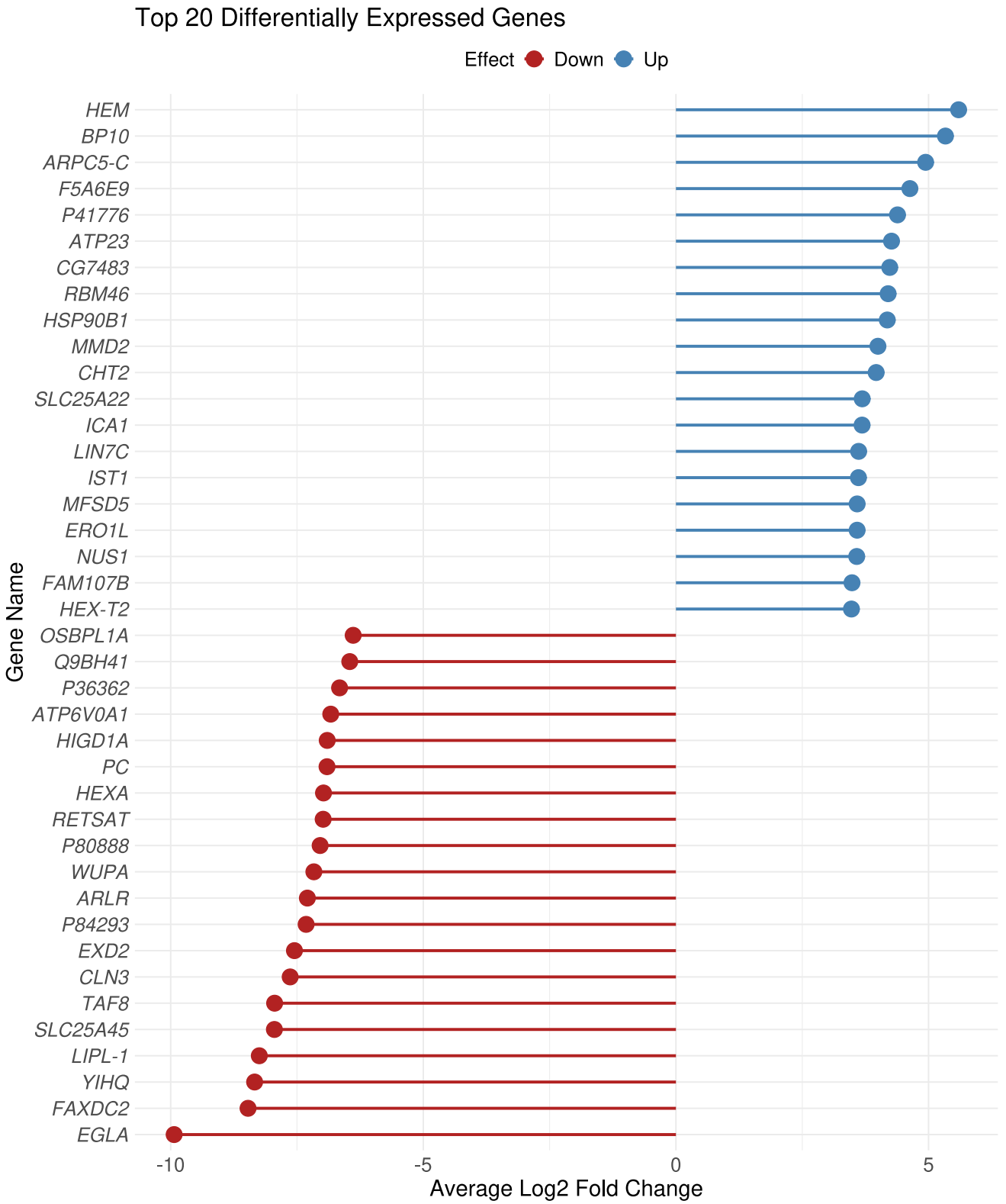

Fig. 3 Top 20 up- and down-regulated differentially expressed transcripts

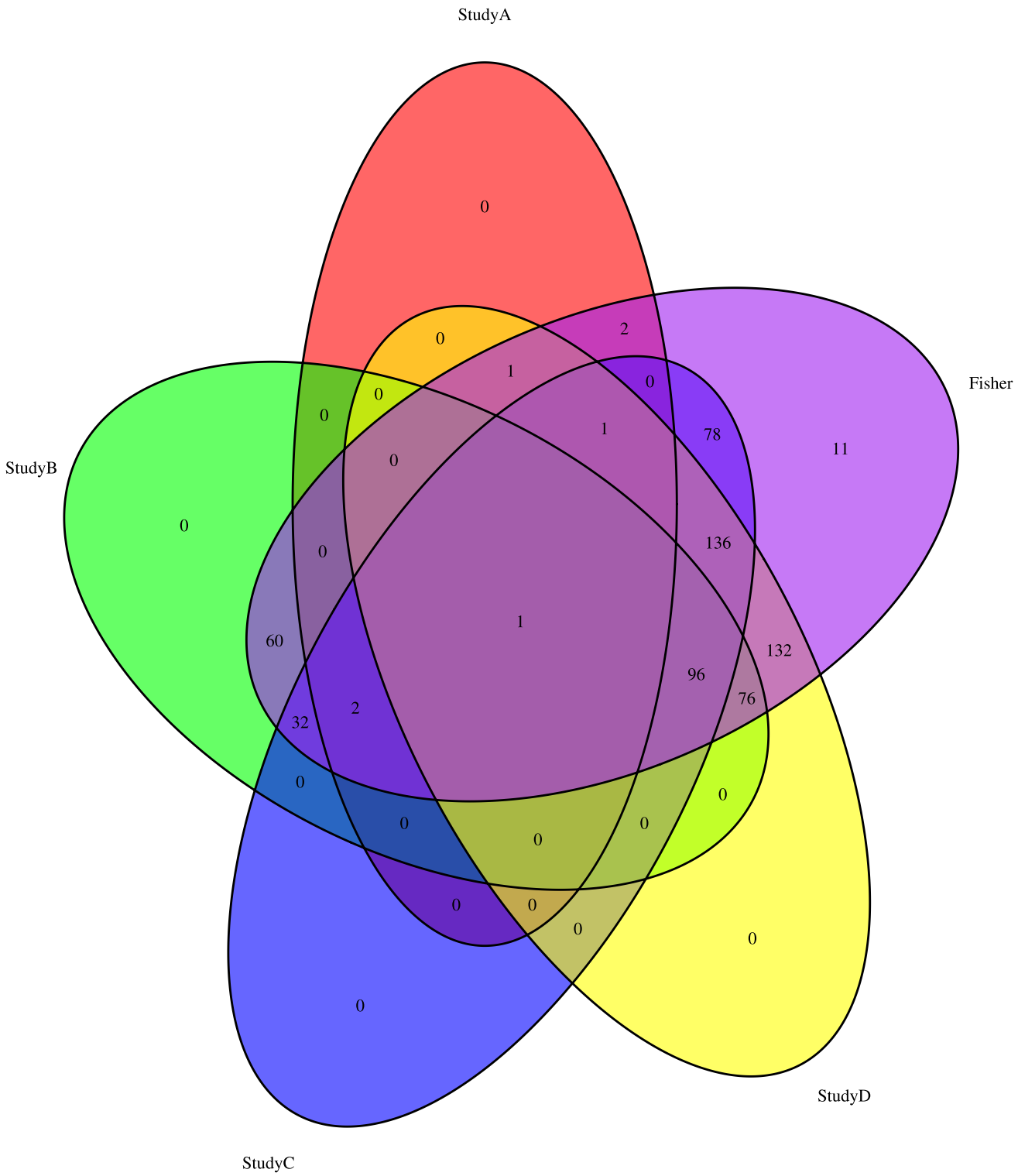

Fig. 4 Venn diagram showing the number of differentially expressed transcripts (DETs) identified from individual studies and meta-analysis based on the Fisher method

(Table 3). The most enriched BP term, mRNA splicing via spliceosome (GO:0000398), suggests potential post-transcriptional regulation in the diseased hepatopancreas. Other significantly enriched terms indicated cytoskeletal reorganization (actin cytoskeleton organization, regulation of cell shape), metabolic reprogramming (carbohydrate metabolism, fatty acid β-oxidation, gluconeogenesis), and oxidative stress response (response to oxidative stress).

Table 2 List of 11 additional differentially expressed transcripts (DETs) identified through meta-analysis

Uniprot ID	Protein names	Organism	Gene Ontology (Biological process)	Effect
A1A4J8	Protein SCO1 homolog, mitochondrial	*Bos taurus*	Mitochondrial cytochrome c oxidase assembly	Up
A1ZAX0	Neuropeptide CCHamide-1 receptor	*Drosophila melanogaster*	G protein-coupled receptor signaling pathway	Down
O02194	Presenilin homolog (DmPS)	*Drosophila melanogaster*	Amyloid-beta formation; apoptotic process	Up
O77245	Nuclear hormone receptor E75	*Metapenaeus ensis*	Cell differentiation; hormone-mediated signaling pathway	Down
P29775	DNA-binding protein D-ETS-4	*Drosophila melanogaster*	Regulation of transcription by RNA polymerase II	Down
Q3T000	Synaptobrevin homolog YKT6	*Bos taurus*	Endoplasmic reticulum to Golgi vesicle-mediated transport	Up
Q5UEM7	Cyclic AMP-responsive element-binding protein 3-like protein 4	*Rattus norvegicus*	Positive regulation of transcription by RNA polymerase II	Up
Q6NV04	2-hydroxyacyl-CoA lyase 2	*Danio rerio*	Embryonic cranial skeleton morphogenesis; fatty acid alpha-oxidation	Down
Q6TNS2	p21-activated protein kinase-interacting protein 1-like	*Danio rerio*	Negative regulation of signal transduction;	Down
Q8N8S7	Protein enabled homolog	*Homo sapiens*	Actin polymerization or depolymerization	Up
Q9N2W7	Probable NADH dehydrogenase [ubiquinone] 1 alpha subcomplex subunit 12	*Caenorhabditis elegans*	Mitochondrial respiratory chain complex I assembly; response to oxidative stress	Up

The 'Effect' column indicates whether each transcript is up- or down-regulated.Underlined UniProt IDs denote genes whose average fold change is < 2, in contrast to the other listed genes, which show an average fold change ≥ 2.

Within MF and CC categories, enrichment of ATP binding, RNA binding, and cellular components such as cytoplasm, mitochondrion, and endoplasmic reticulum highlights major changes in energy utilization and organelle activity associated with the diseased state.

Together, the KEGG and GO analyses indicate that the diseased hepatopancreas undergoes extensive transcriptional reorganization, particularly affecting cellular structure, metabolism, and stress response pathways, which may underlie the observed pathological alterations.

Interaction network of DETs

The DETs were then used to construct the protein–protein interaction (PPI) network which comprised 369 nodes (each node representing a protein/gene) and 1271 edges (PPI enrichment p-value < 1.0e-16). The node degree of each gene (node) in the network ranged from 1 and 39. At least five nodes exhibited a node degree of over 30, and these nodes were considered as hub genes. These hub nodes encode for the following proteins: bifunctional glutamate/proline–tRNA ligase (*GluProRS*: node degree = 39), DNA topoisomerase 2-alpha (*TOP2A*: node degree 37), Phosphoglycerate kinase (*Pgk*: node degree = 36), Cystathionine beta-synthase (*CBS*: node degree = 32), and Small ribosomal subunit protein uS5 (*RPS2*: node degree = 30). Among these five genes, *GluProRS* and *Pgk* are up-regulated and *TOP2A*, *CBS*, and *RPS2* were down-regulated in the meta-analysis.

Furthermore, the PPI network could be divided into 20 modules or communities (clusters). We also observed that only 8/20 modules (Clusters 1–7, and 10) contained 10 or more nodes, and, therefore, only these clusters were selected for enrichment analysis (Fig. 7). Among these modules, cluster 4 was the largest with 93 nodes and 400 edges whereas cluster 10 contained only 14 nodes and 22 edges. We also observed that the hub nodes *TOP2A*, *Pgk*, and *CBS* were present in cluster 4, and the remaining two hub nodes (*GluProRS* and *RPS2*) were found in cluster 1. Additionally, among the 11 new transcripts identified by the meta-analysis, only five were mapped to the network. Specifically, a transcript that encodes nuclear hormone receptor E75 (*E75*) was grouped in cluster 3, whereas two other transcripts that encode cyclic AMP-responsive element-binding protein 3-like protein 4 (*Creb3l4*) and 2-hydroxyacyl-CoA lyase 2 (*ilvbl*) were found in cluster 4. Transcripts encoding protein SCO1 homolog, mitochondrial (*SCO1*) and Synaptobrevin homolog (*YKT6*) were grouped in clusters 5 and 6, respectively.

The enrichment analysis of selected eight modules highlighted the specific functional roles of each individual cluster (Fig. 7). For example, Cluster 1: enriched in gene expression, RNA processing, and mRNA splicing; Cluster

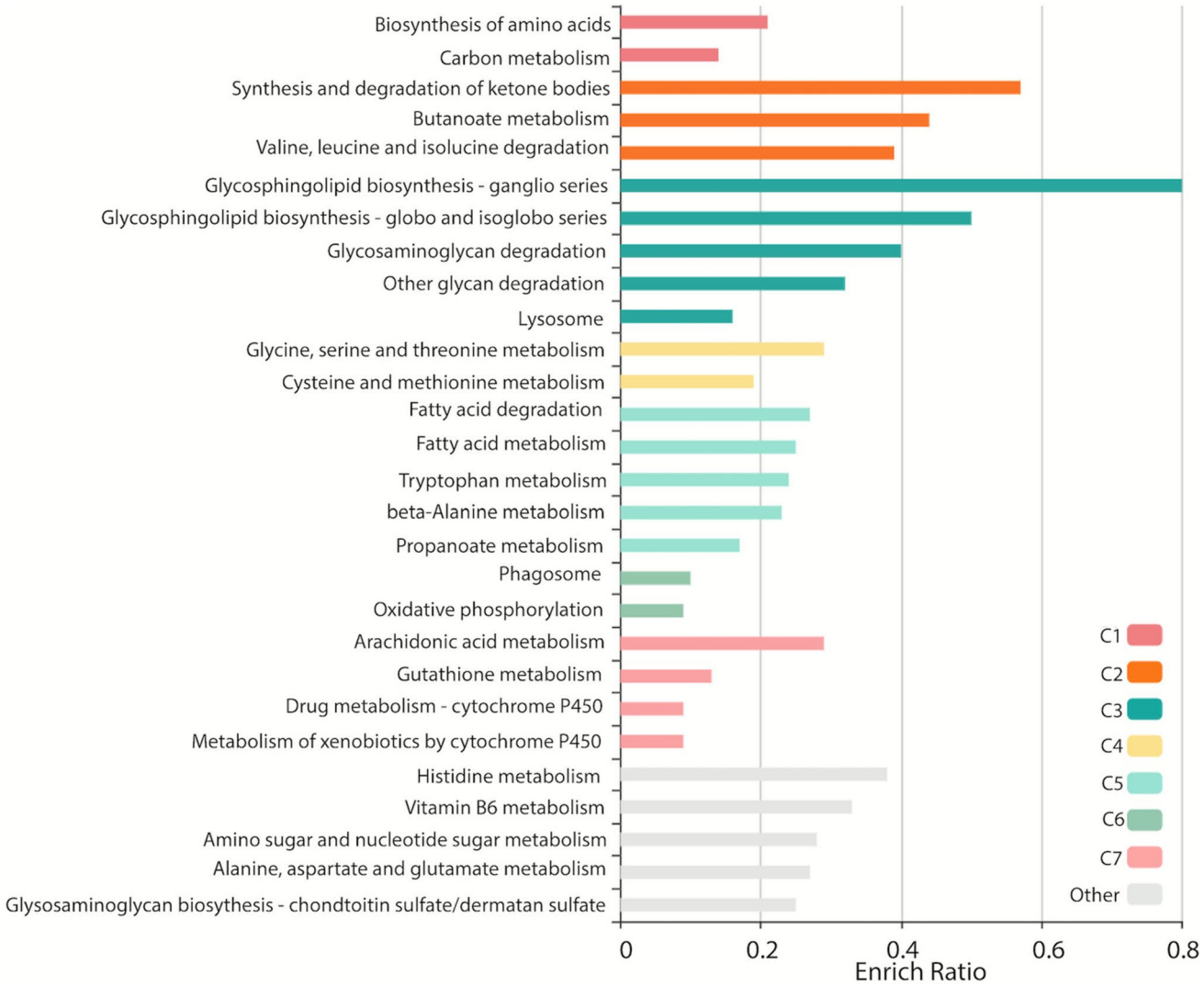

Fig. 5 Bar plot illustrating the enrichment of metabolic pathways based on their enrich ratio

2: exhibited regulatory roles such as cellular regulation, biological regulation, and signal transduction. Cluster 3: involved in protein modification, nitrogen compound metabolic processes, and macromolecule metabolism. Cluster 4 and 7 are enriched with metabolic processes including small molecule metabolism (e.g. organic acids and oxoacids) and lipid metabolism (e.g. phospholipid metabolic processes and glycolipid metabolism). Cluster 5 shows enrichment of processes involving mitochondria such as mitochondrion organization, ion transport, and proton transmembrane transport. In contrast, cluster 6 is enriched in processes related to vesicle-mediated transport, cellular localization, and Golgi vesicle transport. Cluster 10 being the smallest cluster shows enrichment of only three processes related to tRNA metabolic processes, especially tRNA aminoacylation for protein translation. These finding provide a detailed functional characterization of the PPI network and its modular organization, highlighting the biological processes associated with the DETs (Fig. 7 and Figure S1).

Discussion

Transcriptome studies of *E. sinensis* with diseased hepatopancreas have mainly focused on immune-related genes and pathways, and little is known about the overall dynamic changes that undergo during this pathological stress period. In crustaceans, the hepatopancreas serves as both a digestive gland and an immune organ, playing a pivotal role in xenobiotic metabolism and the innate immune system (Gross et al. 2001; Ried et al. 1996; Roux et al. 2002). The enrichment analysis of these individual clusters highlights a network of biological processes essential for cellular functionality, regulation, and adaptation to external

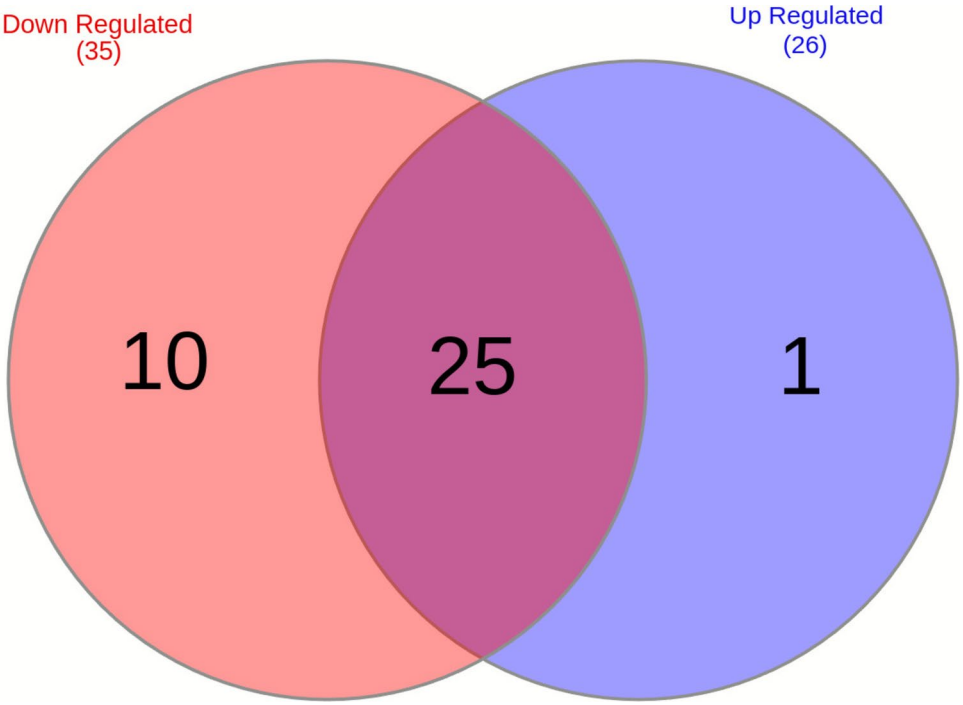

Fig. 6 Venn diagram illustrating the overlap of metabolic pathways between upregulated (blue) and downregulated (red) groups. Numbers within the diagram represent the count of unique or shared pathways

stimuli, particularly during immune responses. These clusters represent components of a cohesive system enabling cells to adapt to environmental changes, balance energy and resource demands, and perform intricate tasks such as signal transduction and gene expression. This integrated perspective underscores the central theme emerging from the clusters:

Core cellular machinery

Clusters 1, 3, 5, and 10 are associated with the biological processes that represent the core cellular machinery. These processes represent the framework of cellular functions, ensuring the availability of essential building blocks such as protein and RNA, while also meeting energy demands. Specifically, these clusters play critical roles in gene expression, RNA processing, and protein modifications, forming the foundation for maintaining cellular functions. The DETs in these clusters are also involved in tRNA metabolism and mitochondrial organization, which are essential for efficient protein synthesis and energy production. Both processes are indispensable for active cellular processes such as immune response. Notably, several down-regulated genes encode ribosomal subunit proteins, including *RPS2*, *RPS7*, *RPS10*, *RPL7*, and *RPL13*. Ribosomal proteins are integral to cellular metabolism, with ribosome synthesis being crucial for cell growth and development. Beyond their role in subunit assembly, these ribosomal proteins also ensure the accurate folding and cleavage of rRNA as highlighted by Badhai et al. (2009).

The hepatopancreas serves as a vital digestive gland in CMCs, playing a crucial role in synthesizing and secreting digestive enzymes (Jiang et al. 2009). It is also essential for the digestion and absorption of nutrients and is responsible for its metabolism (Rosas et al. 1995). These changes are often triggered by stress conditions, including diseases, environmental challenges, or dietary modifications. Previous studies have shown that stressors such as fasting environmental pollutants, or nutrient deficiencies can significantly impact the hepatopancreases' metabolic and immune functions (Guo et al. 2019).

Earlier studies have also suggested that the immune response of crustaceans can be significantly influenced by metabolic demands, pathogens or environmental stressors. Bacterial infections like *Vibrio* spp. and diseases like White Spot Syndrome Virus (WSSV) are known to significantly alter energy and protein metabolism. These alterations indirectly affect ribosomal protein synthesis by disrupting metabolic homeostasis and increasing the demand for energy to fuel immune responses and cellular repair mechanisms (Huang et al. 2020; Betancourt et al. 2024). This dynamic interplay between cellular machinery and immune activation offers potential insights into the biochemical connections between hepatopancreatic disease (HPND) symptoms and its progression.

The up-regulation of mitochondrial import genes, including *Tim13*, *Tim17-B*, *Tim22*, and *TOM7,* indicates increased mitochondrial protein import activity in the hepatopancreas, a key function for maintaining mitochondrial processes under stress. These translocases facilitate the import

of nuclear-encoded proteins into mitochondria, ensuring the proper functioning of oxidative phosphorylation and other mitochondrial processes (Chaudhuri et al. 2020; Sirrenberg et al. 1996). Up-regulation of mitochondrial inner membrane protease ATP23 homolog (*ATP23*) (which processes the ATP6 subunit to assemble ATP synthase), highlights the role of mitochondria in ATP production during energy stress and enhanced energy requirements (Osman et al. 2007; Zeng et al. 2007). Similarly, transporters such as *SLC25A22* (mitochondrial glutamate carrier 1) and *SLC25A51* (NAD+transporter) support energy metabolism and mitochondrial respiration. SLC25A22 refills TCA cycle intermediates while SLC25A51 enhances NAD+transport, critical for maintaining mitochondrial efficiency during stress (Fiermonte et al. 2002). In contrast, down-regulation of SLC25A11 (mitochondrial 2-oxoglutarate/malate carrier), SLC25A40 (mitochondrial glutathione transporter) and mitochondrial Rho GTPase (Miro) suggests disruption in redox homeostasis and mitochondrial dynamics, possibly contributing to hepatopancreatic disease pathology. SLC25A11 mediates metabolite exchange to shield against oxidative stress, while SLC25A40 supports glutathione

Table 3 Enrichment of Gene ontology (GO) terms of DETs identified by meta-analysis

GO term id	GO term description	*P*-value	Corrected *P*-value	GO category
GO:0000398	mRNA splicing, via spliceosome	4.13337647701E-08	6.08019679768E-06	BP
GO:0048749	compound eye development	2.44311626982E-06	0.0002114014137	
GO:0030036	actin cytoskeleton organization	4.37003066666E-06	0.000321415755533	
GO:0008360	regulation of cell shape	1.20321108384E-05	0.000737468126803	
GO:0030866	cortical actin cytoskeleton organization	1.63927912171E-05	0.000893103551125	
GO:0008340	determination of adult lifespan	4.38312265791E-05	0.00195381013024	
GO:0005975	carbohydrate metabolic process	4.68855428575E-05	0.00202848922186	
GO:0006635	fatty acid beta-oxidation	4.97320040043E-05	0.00209016508258	
GO:0000902	cell morphogenesis	0.000111967708691	0.00422319229446	
GO:0051294	establishment of spindle orientation	0.000135517643301	0.00463180308525	
GO:0007430	terminal branching, open tracheal system	0.000137406331349	0.00463180308525	
GO:0007010	cytoskeleton organization	0.00017933126349	0.00561268699136	
GO:0055114	oxidation–reduction process	0.000186872299715	0.00572685735168	
GO:0042417	dopamine metabolic process	0.000208004974433	0.00599951602727	
GO:0045167	asymmetric protein localization involved in cell fate determination	0.000233350285663	0.00657562062672	
GO:0006094	gluconeogenesis	0.000304760344009	0.00786495554452	
GO:0006888	endoplasmic reticulum to Golgi vesicle-mediated transport	0.000317345296747	0.00804853330198	
GO:0007297	ovarian follicle cell migration	0.000429994665812	0.0100400341811	
GO:0042060	wound healing	0.000557104756101	0.0126077091727	
GO:0006979	response to oxidative stress	0.000675797042576	0.0150620825701	
GO:0007035	vacuolar acidification	0.00102023932206	0.0206540232949	
GO:0006468	protein phosphorylation	0.00115704563944	0.0226935218083	
GO:0008593	regulation of Notch signaling pathway	0.00127275385403	0.0236989989782	
GO:0045324	late endosome to vacuole transport	0.00127275385403	0.0236989989782	
GO:0005978	glycogen biosynthetic process	0.00127275385403	0.0236989989782	
GO:1902600	proton transmembrane transport	0.00151232974189	0.027807963129	
GO:0008347	glial cell migration	0.00195820585853	0.0338884802105	
GO:0006487	protein N-linked glycosylation	0.00202573564336	0.0346495015278	
GO:0035293	chitin-based larval cuticle pattern formation	0.00247383198279	0.0387128387945	
GO:0032880	regulation of protein localization	0.00247383198279	0.0387128387945	
GO:0009416	response to light stimulus	0.00247383198279	0.0387128387945	
GO:0007029	endoplasmic reticulum organization	0.00247383198279	0.0387128387945	
GO:0030041	actin filament polymerization	0.00260978780855	0.039173447616	
GO:0072583	clathrin-dependent endocytosis	0.00260978780855	0.039173447616	
GO:0001737	establishment of imaginal disc-derived wing hair orientation	0.0029855801819	0.0414319664866	
GO:0007163	establishment or maintenance of cell polarity	0.0029855801819	0.0414319664866	
GO:0007314	oocyte anterior/posterior axis specification	0.0029855801819	0.0414319664866	
GO:0035088	establishment or maintenance of apical/basal cell polarity	0.00351045637134	0.045209783981	
GO:0018990	ecdysis, chitin-based cuticle	0.00356515065546	0.045209783981	
GO:0002009	morphogenesis of an epithelium	0.00356515065546	0.045209783981	
GO:0043087	regulation of GTPase activity	0.00371035896326	0.0466490430338	
GO:0045214	sarcomere organization	0.00385124536043	0.0476065708	

Table 3 (continued)

GO term id	GO term description	*P*-value	Corrected *P*-value	GO category
GO:0005524	ATP binding	9.53623253884E-10	2.33796634411E-07	MF
GO:0005516	calmodulin binding	2.61840519724E-05	0.00128389134838	
GO:0003723	RNA binding	3.41941523413E-05	0.00160370692074	
GO:0003729	mRNA binding	0.000120016067141	0.00441359086912	
GO:0046961	proton-transporting ATPase activity, rotational mechanism	0.000125187209889	0.00449147282311	
GO:0005515	protein binding	0.000138544755779	0.00463180308525	
GO:0003779	actin binding	0.000163444725605	0.00522667807314	
GO:0004602	glutathione peroxidase activity	0.000783300363799	0.0167293881672	
GO:0052650	NADP-retinol dehydrogenase activity	0.00186750675897	0.0335012492981	
GO:0000287	magnesium ion binding	0.00194619745745	0.0338884802105	
GO:0004674	protein serine/threonine kinase activity	0.00240518715115	0.0387128387945	
GO:0003730	mRNA 3'-UTR binding	0.00260632328244	0.039173447616	
GO:0001664	G protein-coupled receptor binding	0.00298287874328	0.0414319664866	
GO:0004300	enoyl-CoA hydratase activity	0.00351045637134	0.0452097983981	
GO:0051117	ATPase binding	0.00351045637134	0.0452097983981	
GO:0008553	proton-exporting ATPase activity, phosphorylative mechanism	0.00351045637134	0.0452097983981	
GO:0005737	cytoplasm	1.1146122144E-13	8.19797283693E-11	CC
GO:0005739	mitochondrion	1.43542233683E-11	7.03835419158E-09	
GO:0005829	cytosol	7.8608025694E-10	2.31264811592E-07	
GO:0071011	precatalytic spliceosome	5.81974419874E-09	1.22297767376E-06	
GO:0071013	catalytic step 2 spliceosome	1.79212308383E-07	2.02785619717E-05	
GO:0005783	endoplasmic reticulum	5.85126289105E-07	6.1480055091E-05	
GO:0005777	peroxisome	1.72535616038E-06	0.000158624931995	
GO:0012505	endomembrane system	2.43372290403E-05	0.0012344849627	
GO:0005759	mitochondrial matrix	7.86609448458E-05	0.00321417360745	
GO:0005886	plasma membrane	0.000111475158165	0.00422319229446	
GO:0005634	nucleus	0.000159166354591	0.00520297128009	
GO:0030864	cortical actin cytoskeleton	0.000208004974433	0.00599951602727	
GO:0005789	endoplasmic reticulum membrane	0.000369718752565	0.00910363439067	
GO:0000220	vacuolar proton-transporting V-type ATPase, V0 domain	0.000377513050871	0.00910363439067	
GO:0016471	vacuolar proton-transporting V-type ATPase complex	0.000429994665812	0.0100400341811	
GO:0015629	actin cytoskeleton	0.000784723170317	0.0167293881672	
GO:0005769	early endosome	0.00098541807579	0.020416197035	
GO:0005938	cell cortex	0.00122300640723	0.0236716108557	
GO:0005703	polytene chromosome puff	0.00194619745745	0.0338884802105	
GO:0033181	plasma membrane proton-transporting V-type ATPase complex	0.0029855801819	0.0414319664866	
GO:0005793	endoplasmic reticulum-Golgi intermediate compartment	0.0029855801819	0.0414319664866	
GO:0005768	endosome	0.00320280840769	0.043623436738	
GO:0005765	lysosomal membrane	0.00356515065546	0.0452097983981	
GO:0005770	late endosome	0.00385124536043	0.0476065708	

import for antioxidant defense (Lash 2006; Kawase et al. 2022). Among the 11 additional DETs identified in the meta-analysis (Table 2), nuclear hormone receptor E75 (E75) was down-regulated, and protein SCO1 homolog (SCO1), mitochondrial, was up-regulated in clusters 3 and 5, respectively. E75 is an early-responsive gene in the 20-hydroxyecdysone (20E) signaling pathway (Bialecki et al. 2002) and plays key roles in many aspects of crustaceans' development including molting and immune response (Xie et al. 2016). In contrast, SCO1 supports mitochondrial function during stress and is up-regulated under copper induced stress in CMCs (Barresi et al. 2016; Tang et al. 2021). Overall, the DE of these genes reflects the mitochondrial involvement to adapt to heightened metabolic demand and oxidative stress, highlighting their crucial role in maintaining the cellular function during hepatopancreatic disease.

Regulation and signaling

Clusters 2 and 6 are related to processes such as signal transduction, cellular regulation, and vesicle-mediated transport, emphasizing the dynamic cellular response to environmental changes. These processes are vital for systems such as the immune response, which continuously adapts to infection

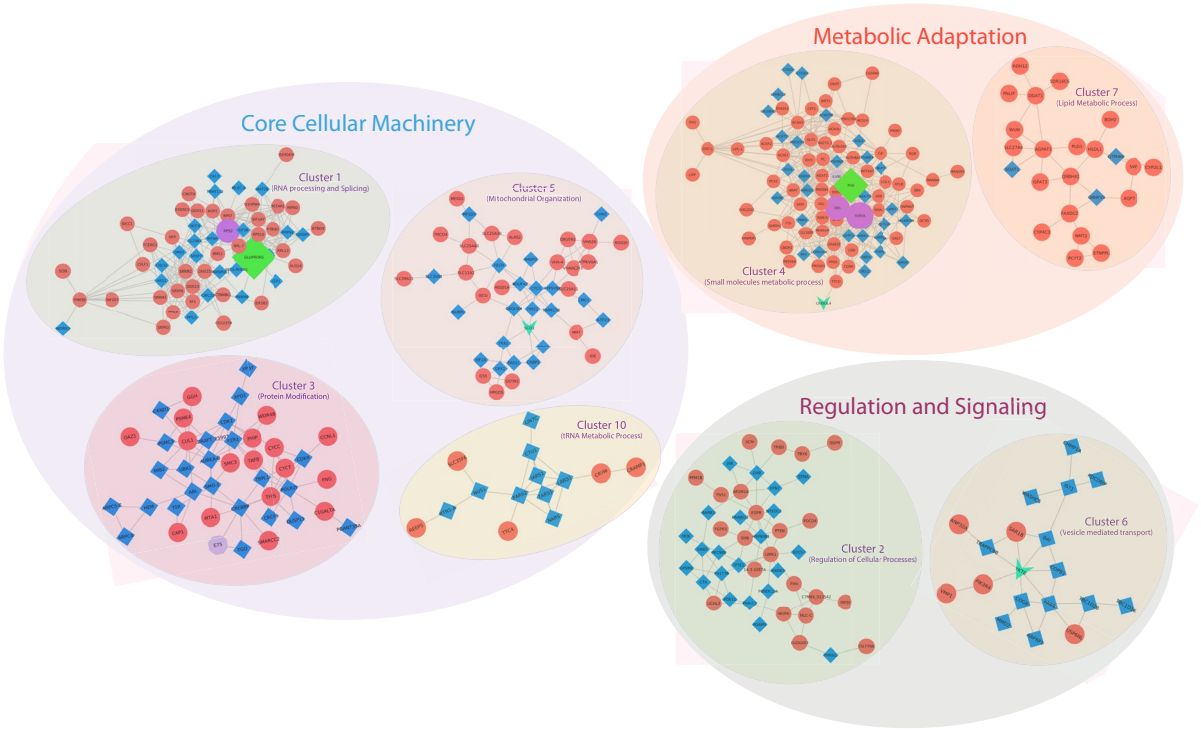

Fig. 7 Functional clustering of gene networks: Core Cellular Machinery, Metabolic Adaptation, and Regulation. This network diagram illustrates the functional clustering of gene networks based on their biological roles. Nodes represent individual genes or proteins, with red circles denoting down-regulated genes and blue diamond showing up-regulated elements. Five enlarged nodes in green and purple represent hubs. Additional genes identified by meta-analysis are represented as either octagon (light-purple; down-regulated), or arrow-shaped (light-blue; up-regulated) nodes. Edges indicate functional interactions between the nodes. The clustering highlights key biological processes

and damage (Wang et al. 2024). Up-regulated kinases, including cAMP-dependent protein kinase catalytic subunit 3 (Protein kinase DC2), MAP/microtubule affinity-regulating kinase 3 (MARK3), phosphorylase b kinase gamma catalytic chain, skeletal muscle/heart isoform (PHKG1), and protein kinase C (PKC), suggest enhanced signaling for stress adaptation and metabolic regulation (Lim et al. 2015). In contrast, the down-regulated kinases such as epidermal growth factor receptor (EGFR), LIM domain kinase 1 (LIMK1), phosphoinositide 3-kinase regulatory subunit 4 (PIK3R4), and phosphorylase b kinase regulatory subunit alpha (CG7766) suggest reduced cell proliferation, cytoskeletal dynamics, and immune modulation (Cheng et al. 2022; Lee et al. 2020).

Vesicle transport processes, including Golgi-mediated transport, were predominant in the cluster 6. These are crucial for immune communication, cytokine release, and antigen presentation (Kaminska et al. 2024). Small GTP-binding proteins (GTPases), such as ADP-ribosylation factor-related protein 1 (ARF) and ras-related protein (RAB6), which regulate vesicle formation, tethering and fusion, were up-regulated, reflecting increased vesicular activity in diseased states (Homma et al. 2021; Ortega et al. 2022). Similarly, up-regulation of soluble N-ethylmaleimide-sensitive factor attachment protein receptor (SNARE) proteins like synaptobrevin homolog YKT6 (YKT6) further underscores the increased trafficking required during immune activation and stress adaptation (Pokrywka et al. 2022; Gao et al. 2018a, b; Zhang et al. 2023) (Table 2). Such processes contribute to hepatopancreatic adaptation to HPND symptoms by enhancing cellular signaling and immune communication under pathological stress.

Metabolic adaptation

Metabolic and immune processes are closely interconnected, as immune activation often triggers metabolic reprogramming to meet increased energy demands (Amo-Aparicio et al. 2024). Key pathways such as lipid, carbohydrate, and small-molecule metabolism, along with ion transport, play essential roles in this adaptive response (Qiu et al. 2023; Chen et al. 2023; Zhang et al. 2022). Lipids, in particular, serve as a primary energy source in *E. sinensis* (Wen et al. 2001). In this study, the down-regulation of transcripts encoding long-chain fatty acid transport protein 4 (FATP-4), long-chain specific acyl-CoA dehydrogenase (LCAD), and long-chain-fatty-acid-CoA ligase 4 (ACSL4) indicates impaired lipid metabolism and reduced energy storage, consistent with previous reports of metabolic disruption in the

diseased hepatopancreas (Liu et al. 2020; Batabyal et al. 2021; Aderinto et al. 2023).

Changes in carbohydrate metabolism further support a metabolic shift during disease progression. The up-regulation of glycolytic enzymes such as hexokinase type 2, triosephosphate isomerase, and phosphoglycerate kinase suggests enhanced glycolysis to meet elevated energy requirements, whereas the down-regulation of gluconeogenic enzymes, including phosphoenolpyruvate carboxykinase (PEPCK) and pyruvate carboxylase, reflects suppressed glucose synthesis from non-carbohydrate sources (Miao et al. 2023). Together, these patterns indicate a reorientation of hepatopancreatic metabolism towards rapid energy production under stress.

As a multifunctional organ integrating digestive, metabolic, and immune functions, the hepatopancreas coordinates diverse biochemical pathways to maintain homeostasis and defense. Processes such as protein modification, lipid metabolism, signal transduction, and vesicle-mediated transport converge to regulate immune signaling and energy balance. Protein modifications (e.g., phosphorylation, ubiquitination, acetylation) modulate key pathways like NF-κB and MAPK, thereby controlling cytokine production and cellular stress responses (Szklarczyk et al. 2023; Tang et al. 2021; Toro-Domínguez et al. 2021). Similarly, vesicle trafficking mediated by small GTPases and SNARE proteins ensures efficient transport of immune mediators, antigen processing, and localized defense activation (UniProt Consortium 2019; Wang et al. 2024; Wen et al. 2001; Xie 2016).

Overall, the observed transcriptional changes highlight a coordinated metabolic adaptation of the hepatopancreas to meet the dual demands of energy production and immune activation during HPND progression. This integrative metabolic–immune framework underscores the hepatopancreas as a central regulator of stress resilience and a promising focus for advancing crustacean disease management and aquaculture sustainability.

Conclusion

The combined DE kinases, vesicle trafficking proteins, and metabolic adjustments illustrate a cellular state geared towards rapid and specialized immune responses. This highlights the hepatopancreas' role not only as a metabolic organ but also as a player in systemic immunity, especially under disease conditions such as bacterial infections or oxidative stress. Moreover, the study enhances our understanding of hepatopancreatic disease in *E. sinensis*, identifying key pathways, hub genes, and novel transcripts. These findings bridge gaps in the literature and provide actionable targets for diagnosis, management, and prevention. Although meta-analysis can identify consistent patterns across studies, it does not establish causal relationships or the functional roles of the identified transcripts. Validation experiments, such as knockdown or overexpression studies are necessary to confirm the roles of key genes and pathways in disease mechanisms. Moreover, as a non-model organism, genomic resources for the *E. sinensis* are limited. This restricts detailed annotation and comparative functional analyses, potentially leaving some novel transcripts uncharacterized. Environmental stressors, including water quality, temperature, and pathogen load vary across studies and may confound the observed transcriptomic responses. A more systematic approach under controlled environmental conditions is needed to isolate specific stress-response pathways. As the industry faces growing challenges from diseases and environmental stressors, utilizing these insights will be essential for ensuring the sustainability and profitability of CMC farming.

Supplementary Information The online version contains supplementary material available at https://doi.org/10.1007/s13258-025-01715-x.

Author contributions AM: Formal analysis, Writing—original draft, Writing—Reviewing and Editing, Methodology, Funding acquisition, Conceptualization, Supervision. NM: Formal analysis, Writing—original draft, Writing—Reviewing and Editing, Methodology, Conceptualization. HA: Validation, Data curation, Visualization. CBK: Resources, Supervision, Conceptualization, Writing—Reviewing and Editing.

Funding This work was supported by the National Research Foundation of Korea (NRF), funded by the Ministry of Science and ICT (2021R1I1A1A01056363).

Data availability All the data is provided in the manuscript.

Declarations

Conflict of interest The author (NM) is an independent freelance consultant in data science and translational research. This work was conducted independently and is not related to, nor supported by, the author's full-time employment. No conflicts of interest are declared.

Consent for publication Not applicable.

Ethical approval and consent to participate Not applicable.

Human and animal rights No animals/humans were used for studies that are the basis of this research.

References

Aderinto N, Abdulbasit MO, Tangmi ADE, Okesanya JO, Mubarak JM (2023) Unveiling the growing significance of metabolism in modulating immune cell function: exploring mechanisms and

implications; a review. Ann Med Surg 85(11):5511–5522. https://doi.org/10.1097/MS9.0000000000001308

Amo-Aparicio J, Dinarello CA, Lopez-Vales R (2024) Metabolic reprogramming of the inflammatory response in the nervous system: the crossover between inflammation and metabolism. Neural Regen Res 19(10):2189–2201. https://doi.org/10.4103/1673-5374.391330

Anger K (1991) Effects of temperature and salinity on the larval development of the Chinese mitten crab *Eriocheir sinensis* (Decapoda: Grapsidae). Mar Ecol Prog 72:103–110

Assenov Y, Ramírez F, Schelhorn SE, Lengauer T, Albrecht M (2008) Computing topological parameters of biological networks. Bioinformatics 24:282–284

Badhai J, Fröjmark AS, Razzaghian HR, Davey E, Schuster J, Dahl N (2009) Posttranscriptional down-regulation of small ribosomal subunit proteins correlates with reduction of 18S rRNA in RPS19 deficiency. FEBS Lett 583(12):2049–2053. https://doi.org/10.1016/j.febslet.2009.05.023

Barresi V, Trovato-Salinaro A, Spampinato G, Musso N, Castorina S, Rizzarelli E, Condorelli DF (2016) Transcriptome analysis of copper homeostasis genes reveals coordinated upregulation of SLC31A1,SCO1, and COX11 in colorectal cancer. FEBS Open Bio 6(8):794–806. https://doi.org/10.1002/2211-5463.12060

Batabyal R, Freishtat N, Hill E, Rehman M, Freishtat R, Koutroulis I (2021) Metabolic dysfunction and immunometabolism in COVID-19 pathophysiology and therapeutics. Int J Obes (Lond) 45(6):1163–1169. https://doi.org/10.1038/s41366-021-00804-7

Betancourt JL, Rodríguez-Ramos T, Dixon B (2024) Pattern recognition receptors in Crustacea: immunological roles under environmental stress. Front Immunol 15:1474512. https://doi.org/10.3389/fimmu.2024.1474512

Bialecki M, Shilton A, Fichtenberg C, Segraves WA, Thummel CS (2002) Loss of the ecdysteroid-inducible E75A orphan nuclear receptor uncouples molting from metamorphosis in Drosophila. Dev Cell 3(2):209–220. https://doi.org/10.1016/s1534-5807(02)00204-6

Bolger AM, Lohse M, Usadel B (2014) Trimmomatic: a flexible trimmer for Illumina sequence data. Bioinformatics 30(15):2114–2120. https://doi.org/10.1093/bioinformatics/btu170

Bray NL, Pimentel H, Melsted P, Pachter L (2016) Near-optimal probabilistic RNA-seq quantification. Nat Biotechnol 34(5):525–527. https://doi.org/10.1038/nbt.3519

Bu D, Luo H, Huo P, Wang Z, Zhang S, He Z, Wu Y, Zhao L, Liu J, Guo J, Fang S, Cao W, Yi L, Zhao Y, Kong L (2021) KOBAS-i: intelligent prioritization and exploratory visualization of biological functions for gene enrichment analysis. Nucleic Acids Res 49(W1):W317–W325. https://doi.org/10.1093/nar/gkab447

Buchfink B, Reuter K, Drost HG (2021) Sensitive protein alignments at tree-of-life scale using DIAMOND. Nat Methods 18(4):366–368. https://doi.org/10.1038/s41592-021-01101-x

Camacho C, Coulouris G, Avagyan V, Ma N, Papadopoulos J, Bealer K, Madden TL (2009) BLAST+: architecture and applications. BMC Bioinformatics 10(1):421. https://doi.org/10.1186/1471-2105-10-421

Chaudhuri M, Darden C, Gonzalez FS, Singha UK, Quinones L, Tripathi A (2020) Tim17 updates: a comprehensive review of an ancient mitochondrial protein translocator. Biomolecules 10(12):1643. https://doi.org/10.3390/biom10121643

Chen X, Wang J, Yue W, Liu J, Wang C (2017) Hepatopancreas transcriptome analysis of Chinese mitten crab (*Eriocheir sinensis*) with white hepatopancreas syndrome. Fish Shellfish Immunol 70:302–307. https://doi.org/10.1016/j.fsi.2017.08.031

Chen W, Zhao H, Li Y (2023) Mitochondrial dynamics in health and disease: mechanisms and potential targets. Signal Transduct Target Ther 8(1):333. https://doi.org/10.1038/s41392-023-01547-9

Cheng YX, Xu WB, Dong WR, Zhang YM, Li BW, Chen DY, Xiao Y, Guo XL, Shu MA (2022) Identification and functional analysis of epidermal growth factor receptor (EGFR) from *Scylla paramamosain*: the first evidence of two EGFR genes in animal and their involvement in immune defense against pathogen infection. Mol Immunol 151:143–157. https://doi.org/10.1016/j.molimm.2022.08.004

Cho H, Kim H, Na D, Kim SY, Jo D, Lee D (2016) Meta-analysis method for discovering reliable biomarkers by integrating statistical and biological approaches: an application to liver toxicity. Biochem Biophys Res Commun 471(2):274–281. https://doi.org/10.1016/j.bbrc.2016.01.082

Dai LS, Abbas MN, Kausar S, Zhou Y (2017) Transcriptome analysis of hepatopancraes of *Procambarus clarkii* challenged with polyriboinosinic polyribocytidylic acid (poly I:C). Fish Shellfish Immunol 71:144–150. https://doi.org/10.1016/j.fsi.2017.10.010

Ding Z, Meng Q, Liu H, Yuan S, Zhang F, Sun M, Zhao Y, Shen M, Zhou G, Pan J, Xue H, Wang W (2016) First case of hepatopancreatic necrosis disease in pond-reared Chinese mitten crab, *Eriocheir sinensis*, associated with microsporidian. J Fish Dis 39(9):1043–1051. https://doi.org/10.1111/jfd.12437

Fan LF, Wang L, Wang ZL (2019) Proteomic characterization of the hepatopancreas in the Pacific white shrimp *Litopenaeus vannamei* under cold stress: revealing the organism homeostasis mechanism. Fish Shellfish Immunol 92:1209–1222. https://doi.org/10.1016/j.fsi.2019.06.037

Fiermonte G, Palmieri L, Todisco S, Agrimi G, Palmieri F, Walker JE (2002) Identification of the mitochondrial glutamate transporter. Bacterial expression, reconstitution, functional characterization, and tissue distribution of two human isoforms. J Biol Chem 277(22):19289–19294. https://doi.org/10.1074/jbc.M201572200

Fisher, R.A. *Statistical Methods for Research Workers*; Oliver and Boyd: Edinburgh, UK, 1925.

Fisher RA (1992) Statistical Methods for Research Workers. In: Kotz S, Johnson NL (eds) Breakthroughs in Statistics. Springer Series in Statistics. Springer, New York, NY. https://doi.org/10.1007/978-1-4612-4380-9_6

Food and Agriculture Organization (FAO). https://www.fao.org/fishery/en/aqspecies/3466/en.

Fu L, Niu B, Zhu Z, Wu S, Li W (2012) CD-HIT: accelerated for clustering the next-generation sequencing data. Bioinformatics 28(23):3150–3152. https://doi.org/10.1093/bioinformatics/bts565

Gao T, Xu Y, Wang K, Deng Y, Yang Y, Lu Q, Pan J, Xu Z (2018a) Comparative LC-MS based non-targeted metabolite profiling of the Chinese mitten crab *Eriocheir sinensis* suffering from hepatopancreatic necrosis disease (HPND). Aquaculture 491:338–345. https://doi.org/10.1016/j.aquaculture.2018.03.030

Gao J, Reggiori F, Ungermann C (2018b) A novel in vitro assay reveals SNARE topology and the role of Ykt6 in autophagosome fusion with vacuoles. J Cell Biol 217(1):3670–3682. https://doi.org/10.1083/jcb.201804039

Gross PS, Bartlett TC, Browdy CL, Chapman RW, Warr GW (2001) Immune gene discovery by expressed sequence tag analysis of hemocytes and hepatopancreas in the Pacific White Shrimp, *Litopenaeus vannamei*, and the Atlantic White Shrimp. L Setiferus Dev Comp Immunol 25(7):565–577. https://doi.org/10.1016/s0145-305x(01)00018-0. (**PMID: 11472779**)

Guo H, Tang D, Shi X et al (2019) Comparative transcriptome analysis reveals the expression and characterization of digestive enzyme genes in the hepatopancreas of the Chinese mitten crab. Fish Sci 85:979–989. https://doi.org/10.1007/s12562-019-01358-4

Haas BJ, Papanicolaou A, Yassour M, Grabherr M, Blood PD, Bowden J, Couger MB, Eccles D, Li B, Lieber M, MacManes MD, Ott M, Orvis J, Pochet N, Strozzi F, Weeks N, Westerman R, William T, Dewey CN, Henschel R, LeDuc RD, Friedman N, Regev A

(2013) De novo transcript sequence reconstruction from RNA-seq using the Trinity platform for reference generation and analysis. Nat Protoc 8(8):1494–1512. https://doi.org/10.1038/nprot.2013.084

Homma Y, Hiragi S, Fukuda M (2021) Rab family of small GTPases: an updated view on their regulation and functions. FEBS J 288(1):36–55. https://doi.org/10.1111/febs.15453

Hong Y, Huang Y, Yan G, Huang Z (2019) Effects of deltamethrin on the antioxidant defense and heat shock protein expression in Chinese mitten crab, *Eriocheir sinensis*. Environ Toxicol Pharmacol 66:1–6. https://doi.org/10.1016/j.etap.2018.12.012

Huang Z, Aweya JJ, Zhu C, Tran NT, Hong Y, Li S, Yao D, Zhang Y (2020) Modulation of crustacean innate immune response by amino acids and their metabolites: inferences from other species. Front Immunol 11:574721. https://doi.org/10.3389/fimmu.2020.574721

Huerta-Cepas J, Forslund K, Coelho LP, Szklarczyk D, Jensen LJ, von Mering C, Bork P (2017) Fast genome-wide functional annotation through orthology assignment by eggNOG-Mapper. Mol Biol Evol 34(8):2115–2122. https://doi.org/10.1093/molbev/msx148

Jiang H, Cai YM, Chen LQ, Zhang XW, Hu SN, Wang Q (2009) Functional annotation and analysis of expressed sequence tags from the hepatopancreas of Mitten Crab (*Eriocheir sinensis*). Mar Biotechnol (NY) 11(3):317–326. https://doi.org/10.1007/s10126-008-9146-1

Kaminska P, Tempes A, Scholz E, Malik AR (2024) Cytokines on the way to secretion. Cytokine Growth Factor Rev 79:52–65. https://doi.org/10.1016/j.cytogfr.2024.08.003

Kawase A, Hatanaka M, Matsuda N, Shimada H, Iwaki M (2022) Slc25a39 and Slc25a40 expression in mice with bile duct ligation or lipopolysaccharide treatment. Int J Mol Sci 23(15):8573. https://doi.org/10.3390/ijms23158573

Langmead B, Salzberg SL (2012) Fast gapped-read alignment with Bowtie 2. Nat Methods 9(4):357–359. https://doi.org/10.1038/nmeth.1923

Lash LH (2006) Mitochondrial glutathione transport: physiological, pathological and toxicological implications. Chem Biol Interact 163(27):54–67. https://doi.org/10.1016/j.cbi.2006.03.001

Lee KJ, Kim Y, Kim MS, Ju HM, Choi B, Lee H, Jeoung D, Moon KW, Kang D, Choi J, Yook JI, Hahn JH (2020) CD99-PTPN12 axis suppresses actin cytoskeleton-mediated dimerization of epidermal growth factor receptor. Cancers (Basel) 12(9):2895. https://doi.org/10.3390/cancers12102895

Li X, Cui Z, Liu Y, Song C, Shi G (2013) Transcriptome analysis and discovery of genes involved in immune pathways from hepatopancreas of microbial challenged mitten crab *Eriocheir sinensis*. PLoS ONE 8(7):e68233. https://doi.org/10.1371/journal.pone.0068233

Lim PS, Sutton CR, Rao S (2015) <article-title update="added"> Protein kinase <scp>C</scp> in the immune system: from signalling to chromatin regulation. Immunology 146(4):508–522. https://doi.org/10.1111/imm.12510

Liu LS, Yang ZY, Zhang YL, Zhang FX, Cai HG, Hu K, Yang XL (2017) Research progress on epidemic situation and pathology of *Eriocheir sinensi* "shuibiezi" disease in 2016. Sci Fish Farm 4:61–62 **((in Chinese))**

Liu JD, Liu WB, Zhang CY, Xu CY, Zheng XC, Zhang DD, Chi C (2020) Dietary glutathione supplementation enhances antioxidant activity and protects against lipopolysaccharide-induced acute hepatopancreatic injury and cell apoptosis in Chinese mitten crab, *Eriocheir sinensis*. Fish Shellfish Immunol 97:440–454. https://doi.org/10.1016/j.fsi.2019.12.049

Liu X, Jiang H, Ye B, Qian H, Guo Z, Bai H, Gong J, Feng J, Ma K (2021) Comparative transcriptome analysis of the gills and hepatopancreas from *Macrobrachium rosenbergii* exposed to the heavy metal Cadmium (Cd2+). Sci Rep 11(9):16140. https://doi.org/10.1038/s41598-021-95709-w

Malik A, Kim CB (2021) Role of transportome in the gills of Chinese mitten crabs in response to salinity change: a meta-analysis of RNA-Seq datasets. Biology (Basel) 10(8):39. https://doi.org/10.3390/biology10010039

Marot G, Jaffr'ezic F, Rau A (2020) metaRNASeq: Differential meta-analysis of RNA-seq data. Dim (param) 2020:1–3

Miao M, Li S, Liu Y, Yu Y, Li F (2023) Transcriptome analysis on hepatopancreas reveals the metabolic dysregulation caused by *Vibrio parahaemolyticus* infection in *Litopenaeus vannamei*. Biology (Basel) 12(9):417. https://doi.org/10.3390/biology12030417

Olsvik PA, Lie KK, Hevrøy EM (2007) Do anesthetics and sampling strategies affect transcription analysis of fish tissues? BMC Mol Biol 8(8):48. https://doi.org/10.1186/1471-2199-8-48

Ortega MA, Fraile-Martinez O, Garcia-Montero C, Alvarez-Mon MA, Gomez-Lahoz AM, Albillos A, Lahera G, Quintero J, Monserrat J, Guijarro LG, Alvarez-Mon M (2022) An updated view of the importance of vesicular trafficking and transport and their role in immune-mediated diseases: potential therapeutic interventions. Membranes (Basel) 12(25):552. https://doi.org/10.3390/membranes12060552

Osman C, Wilmes C, Tatsuta T, Langer T (2007) <article-title update="added"> Prohibitins Interact Genetically with Atp23, a Novel Processing Peptidase and Chaperone for the F_1F_O-ATP Synthase. Mol Biol Cell 18(2):627–635. https://doi.org/10.1091/mbc.e06-09-0839

Pan Z, Song X, Hu X, Xue R, Cao G et al (2017) Pathological changes and risk factors of hepatopancreas necrosis disease of mitten crab, *Eriocheir sinensis*. Fish Aqua J 8:220. https://doi.org/10.4172/2150-3508.1000220

Piras IS, Manchia M, Huentelman MJ, Pinna F, Zai CC, Kennedy JL, Carpiniello B (2019) Peripheral biomarkers in schizophrenia: a meta-analysis of microarray gene expression datasets. Int J Neuropsychopharmacol 22(3):186–193. https://doi.org/10.1093/ijnp/pyy103

Pokrywka NJ, Bush S, Nick SE (2022) The R-SNARE Ykt6 is required for multiple events during oogenesis in Drosophila. Cells & Development 169:203759. https://doi.org/10.1016/j.cdev.2021.203759

Qiu S, Cai Y, Yao H, Lin C, Xie Y, Tang S, Zhang A (2023) Small molecule metabolites: discovery of biomarkers and therapeutic targets. Signal Transduct Target Ther 8(1):132. https://doi.org/10.1038/s41392-023-01399-3

Rau A, Marot G, Jaffrézic F (2014) Differential meta-analysis of RNA-seq data from multiple studies. BMC Bioinformatics 15(1):91. https://doi.org/10.1186/1471-2105-15-91

Ried C, Wahl C, Miethke T, Wellnhofer G, Landgraf C, Schneider-Mergener J, Hoess A (1996) High affinity endotoxin-binding and neutralizing peptides based on the crystal structure of recombinant Limulus anti-lipopolysaccharide factor. J Biol Chem 271(45):28120–28127. https://doi.org/10.1074/jbc.271.45.28120

Robinson MD, McCarthy DJ, Smyth GK (2010) edgeR: a Bioconductor package for differential expression analysis of digital gene expression data. Bioinformatics 26(1):139–140. https://doi.org/10.1093/bioinformatics/btp616

Rosas C, Bolongaro-Crevenna A, Sanchez A, Gaxiola G, Soto L, Escobar E (1995) Role of Digestive Gland in the Energetic Metabolism of Penaeus setiferus. Biol Bull 189(2):168–174. https://doi.org/10.2307/1542467

Roux MM, Pain A, Klimpel KR, Dhar AK (2002) The lipopolysaccharide and beta-1,3-glucan binding protein gene is upregulated in white spot virus-infected shrimp (Penaeus stylirostris). J Virol 76(14):7140–7149. https://doi.org/10.1128/jvi.76.14.7140-7149.2002

Seppey M, Manni M, Zdobnov EM (2019) BUSCO: assessing genome assembly and annotation completeness. Methods Mol Biol 1962:227–245. https://doi.org/10.1007/978-1-4939-9173-0_14

Shannon P, Markiel A, Ozier O, Baliga NS, Wang JT, Ramage D, Amin N, Schwikowski B, Ideker T (2003) Cytoscape: a software environment for integrated models of biomolecular interaction networks. Genome Res 13(11):2498–2504. https://doi.org/10.1101/gr.1239303

Shen H, Zang Y, Song K, Ma Y, Dai T, Serwadda A (2017) A metatranscriptomics survey reveals changes in the microbiota of the Chinese mitten crab *Eriocheir sinensis* infected with hepatopancreatic necrosis disease. Front Microbiol 8:732. https://doi.org/10.3389/fmicb.2017.00732

Sirrenberg C, Bauer MF, Guiard B, Neupert W, Brunner M (1996) Import of carrier proteins into the mitochondrial inner membrane mediated by Tim22. Nature 384(6609):582–585. https://doi.org/10.1038/384582a0

Su G, Kuchinsky A, Morris JH, States DJ, Meng F (2010) GLay: community structure analysis of biological networks. Bioinformatics 26(24):3135–3137. https://doi.org/10.1093/bioinformatics/btq596

Sui L, Zhang F, Wang X et al (2009) Genetic diversity and population structure of the Chinese mitten crab *Eriocheir sinensis* in its native range. Mar Biol 156:1573–1583

Szklarczyk D, Kirsch R, Koutrouli M, Nastou K, Mehryary F, Hachilif R, Gable AL, Fang T, Doncheva NT, Pyysalo S, Bork P, Jensen LJ, von Mering C (2023) The STRING database in 2023: protein-protein association networks and functional enrichment analyses for any sequenced genome of interest. Nucleic Acids Res 51(D1):D638–D646. https://doi.org/10.1093/nar/gkac1000

Tang D, Liu R, Shi X, Shen C, Bai Y, Tang B, Wang Z (2021) Toxic effects of metal copper stress on immunity, metabolism and pathologic changes in Chinese mitten crab (*Eriocheir japonica sinensis*). Ecotoxicology 30(4):632–642. https://doi.org/10.1007/s10646-021-02367-9

Toro-Domínguez D, Villatoro-García JA, Martorell-Marugán J, Román-Montoya Y, Alarcón-Riquelme ME, Carmona-Sáez P (2021) A survey of gene expression meta-analysis: methods and applications. Brief Bioinform 22(2):1694–1705. https://doi.org/10.1093/bib/bbaa019

UniProt Consortium (2019) UniProt: a worldwide hub of protein knowledge. Nucleic Acids Res 47(D1):D506–D515. https://doi.org/10.1093/nar/gky1049

Wang W, Wu X, Liu Z, Zheng H, Cheng Y (2014) Insights into hepatopancreatic functions for nutrition metabolism and ovarian development in the crab *Portunus trituberculatus*: gene discovery in the comparative transcriptome of different hepatopancreas stages. PLoS ONE 9(1):e84921. https://doi.org/10.1371/journal.pone.0084921

Wang C, Zhou Y, Lv D, Ge Y, Li H, You Y (2019) Change in the intestinal bacterial community structure associated with environmental microorganisms during the growth of Eriocheir sinensis. Microbiologyopen 8(5):e00727. https://doi.org/10.1002/mbo3.727

Wang QJ, Zhang BY, Jiang XD, Long XW, Zhu WL, Xu YP, Wu M, Zhang DM (2021) Comparison on nutritional quality of adult female Chinese mitten crab (*Eriocheir sinensis*) with different colored hepatopancreases. J Food Sci 86(5):2075–2090. https://doi.org/10.1111/1750-3841.15664

Wang S, Zhang Y, Zhang L, Huang Y, Zhang J, Zhang K, Huang Y, Su G, Chen L, Yan B (2024) Unraveling the complex dynamics of signaling molecules in cellular signal transduction. PNAS Nexus 3(1):pgae020. https://doi.org/10.1093/pnasnexus/pgae020

Wen X-B, Chen L-Q, Ai C-X, Jiang H-B (2001) Standard metabolism of the juvenile crab *Eriocheir sinensis*. Zool Res 22(5):425–428

Xie X, Zhou Y, Liu M, Tao T, Jiang Q, Zhu D (2016) The nuclear receptor E75 from the swimming crab, *Portunus trituberculatus*: cDNA cloning, transcriptional analysis, and putative roles on expression of ecdysteroid-related genes. Comp Biochem Physiol B Biochem Mol Biol 200:69–77. https://doi.org/10.1016/j.cbpb.2016.06.004

Yang ZY, Zhang YL, Hu K, Liu LS, Cai HG, Zhang FX et al (2018) Etiological and histopathological study on hepatopancreatic necrosis syndrome in *Eriocheir sinesis*. Acta Hydrobiol Sin 42(1):17–22

Yang Z, Zhou J, Wei B, Cheng Y, Zhang L, Zhen X (2019) Comparative transcriptome analysis reveals osmotic-regulated genes in the gill of Chinese mitten crab (*Eriocheir sinensis*). PLoS ONE 14(1):e0210469. https://doi.org/10.1371/journal.pone.0210469

Yang Z, Hu K, Hou Y, Wang Y, Yao Y, Lei X, Yan B, Jiang Q, Xiong C, Xu L, Zeng L (2020) Transcriptome analysis of hepatopancreas of *Eriocheir sinensis* with hepatopancreatic necrosis disease (HPND). PLoS ONE 15(2):e0228623. https://doi.org/10.1371/journal.pone.0228623

Zeng X, Neupert W, Tzagoloff A (2007) The metalloprotease encoded by ATP23 has a dual function in processing and assembly of subunit 6 of mitochondrial ATPase. Mol Biol Cell 18(2):617–626. https://doi.org/10.1091/mbc.e06-09-0801

Zhang D, Qi T, Liu J, Liu Q, Jiang S, Zhang H, Wang Z, Ding G, Tang B (2018) Adaptively differential expression analysis in gill of Chinese mitten crabs (*Eriocheir japonica sinensis*) associated with salinity changes. Int J Biol Macromol 120:2242–2246. https://doi.org/10.1016/j.ijbiomac.2018.08.054

Zhang J, Dai W, Chen Y (2022) Editorial: the roles of lipids in immunometabolism: the crosstalk between lipid metabolisms and inflammation. Front Cardiovasc Med 9:938535. https://doi.org/10.3389/fcvm.2022.938535

Zhang X, G Dapar ML, Zhang X, Chen Y (2023) A pan-cancer analysis of the oncogenic role of YKT6 in human tumors. Medicine Baltimore 102(15):e33546. https://doi.org/10.1097/MD.0000000000033546